ORGANIC CHEMISTRY

Couple-close: Unified approach to semisaturated cyclic scaffolds

Jiaxin Xie[1], William Y. Zhao[1], Johnny Z. Wang[1], William L. Lyon[1], Noriyuki Takanashi[1], Alice Long[1], Taylor M. Sodano[2], Christopher B. Kelly[3], Marian C. Bryan[2], David W. C. MacMillan[1]*

Couple-close as a synthetic paradigm has the potential to change the way that synthetic organic chemists approach cyclic scaffold construction. One class of cyclic molecules that has been increasingly sought after is semisaturated cyclic scaffolds, whose specific blend of Csp^2- and Csp^3-hybridized components confers distinct properties to these species. However, existing methods to construct these scaffolds are limited, often relying on arene saturation or annulations that require lengthy de novo syntheses. Herein, we describe a unified and highly modular couple-close strategy for the synthesis of semisaturated scaffolds. This approach installs bifunctional linkers onto aromatic rings through a range of bond-forming reactions, and subsequent cyclization furnishes semisaturated bicyclic adducts. Key to this approach is a mechanistically distinct cobalt-catalyzed dehydrogenative radical cyclization that proceeds efficiently even on electronically unbiased arenes, enabling a broad substrate scope under mild reaction conditions.

Since the advent of the Diels-Alder reaction, the development of chemical transformations that allow rapid and modular access to complex cyclic and polycyclic scaffolds has been central to the field of organic synthesis. Historically, the generation of semisaturated polycycles, a mainstay structural core of agro- and medicinal chemistry, has required lengthy de novo synthetic sequences involving bespoke intermediates, functional group interconversions, and redox manipulations. Recently, our laboratory introduced the concept of couple-close, an aliphatic-aromatic ring-forming protocol that allows modular access to diverse polycyclic rings in only two chemical steps from broadly available starting materials such as diols and pyridyl bromides (*1*). By unifying ring synthesis under a single, expedited strategy involving a sequence of any "couple" step followed by a "close" step from easily accessible precursors, couple-close as a synthetic paradigm has the potential to obviate many synthetic bottlenecks associated with traditional polycyclic ring formation.

Semisaturated bicycles (Fig. 1A) have recently attracted substantial research interest (*2*–*7*) because they are ideally positioned to balance classical arene interactions with the advantages of higher sp^3 content. Additionally, the saturated component of these scaffolds restricts the conformation of the C(sp^3) fragment, conferring additional favorable properties to semisaturated bicycles (*8*, *9*). Despite their desirability, these semisaturated scaffolds remain underrepresented in drug discovery programs and fragment libraries (*10*, *11*). This gap stems from the synthetic challenges associated with their construction. Current approaches rely on substrate-dependent dearomative hydrogenation (*7*) or cationic (*12*–*14*) and radical (*15*–*23*) annulations. In each case, lengthy de novo synthesis of bespoke cyclization precursors limits the accessibility of this chemotype. Our initial demonstration of couple-close as a synthetic paradigm uses metallaphotoredox catalysis to achieve the initial bond-forming "couple" step, followed by a Minisci-type "close" step into electron-deficient aza-heteroarenes, which are well-established radical acceptors (Fig. 1A).

This strategy greatly accelerates access to pyridyl-based semisaturated scaffolds but has key scope limitations because only 3-pyridyl–type heteroaryl bromides can be reliably used as the arene substrate. This limitation, arising from inefficient, substrate-dependent radical cyclization into arene rings, necessitates reliance on Minisci radical cyclization. The efficiency of this process derives from a lowest unoccupied molecular orbital (LUMO)–lowering Lewis acid coordination effect, which shifts the LUMO from an inaccessible +3.45 eV to a reactive −3.05 eV (*23*). However, <10% of commercial aryl bromides (*24*) fall under the purview of a Lewis acid–enabled, Minisci couple-close sequence (Fig. 1A). Common aryl bromides not amenable to Minisci cyclization, including benzenes, 2- or 4-pyridyl heterocycles, and 5-membered heterocycles, are not competent substrates for this couple-close platform. These three categories account for >90% of commercial aryl bromides (*24*), so most of semisaturated bicyclic chemical space remains inaccessible by couple-close (*1*) (Fig. 1B). To access the full range of semisaturated bicycles, a truly general couple-close platform is needed. Key to this generality is the development of a substrate-independent radical cyclization mechanism.

Radical cyclization has traditionally relied on a stepwise oxidation-deprotonation sequence (*1*, *15*, *16*, *19*) that is highly dependent on arene electronics and substitution pattern, limiting its scope and general synthetic utility. Access to diverse semisaturated chemical space therefore requires a mechanistic approach that decouples the "close" step from these constraints. Along these lines, hydrogen atom transfer (HAT) can achieve the same outcome through a single, concerted, and substrate-independent mechanism. Indeed, cobalt-catalyzed HAT has been used to drive radical cyclization into arenes. Beautiful work from the Shenvi (*21*, *25*) and Matsunaga (*22*) laboratories demonstrated that a single cobalt catalyst can generate radicals from alkenes through a metal-hydride hydrogen atom transfer (MHAT) mechanism. These radicals then cyclize into arenes driven by cobalt-mediated HAT (Fig. 1C). In these studies, the resulting Co–H hydrogen species has only been shown to be quenched by MHAT into an alkene. Consequently, the scope of previous applications of this strategy has been limited to custom-synthesized alkene precursors with inherent constraints on the accessible substitution patterns of the resulting semisaturated scaffold. Herein, we leverage a previously underutilized Co–H hydrogen evolution mechanism (*26*, *27*), in combination with the well-established Co-HAT activity (*28*–*33*), to develop a mild, general radical cyclization platform for the rapid construction of semisaturated aromatic scaffolds (Fig. 1D). Although previous work (*33*) has used hydrogen evolution to quench Co–H species, this strategy has not previously been applied to C–C bond-forming radical cyclization.

Unlike previous approaches, this reaction is general and imposes no substrate restrictions, expanding entry to semisaturated scaffolds, including previously noncompatible benzenes, 2- and 4-aza-arenes, and 5-membered heterocycles. The substrate-agnostic nature of this general couple-close platform is demonstrated through 59 examples in the main text and an additional 23 examples in the supplementary materials across 12 distinct classes of arenes and heteroarenes.

Reaction design

The major barrier to developing a truly general couple-close platform is the difficulty of promoting radical addition into unactivated aromatic rings. Although radical addition into arenes has been extensively studied (*15*–*22*), substantial challenges remain. Notably, disruption of aromaticity renders the process reversible (*34*, *35*), often in favor of the "open" form. This predisposes the radical toward unproductive pathways such as HAT or disproportionation (*36*). Previous studies relied on swift oxidation of the cyclized pro-aromatic

[1]Merck Center for Catalysis at Princeton University, Princeton, NJ, USA. [2]Global Discovery Chemistry, Johnson & Johnson Innovative Medicine, Spring House, PA, USA. [3]Discovery Process Research, Johnson & Johnson Innovative Medicine, Spring House, PA, USA.
*Corresponding author. Email: dmacmill@princeton.edu

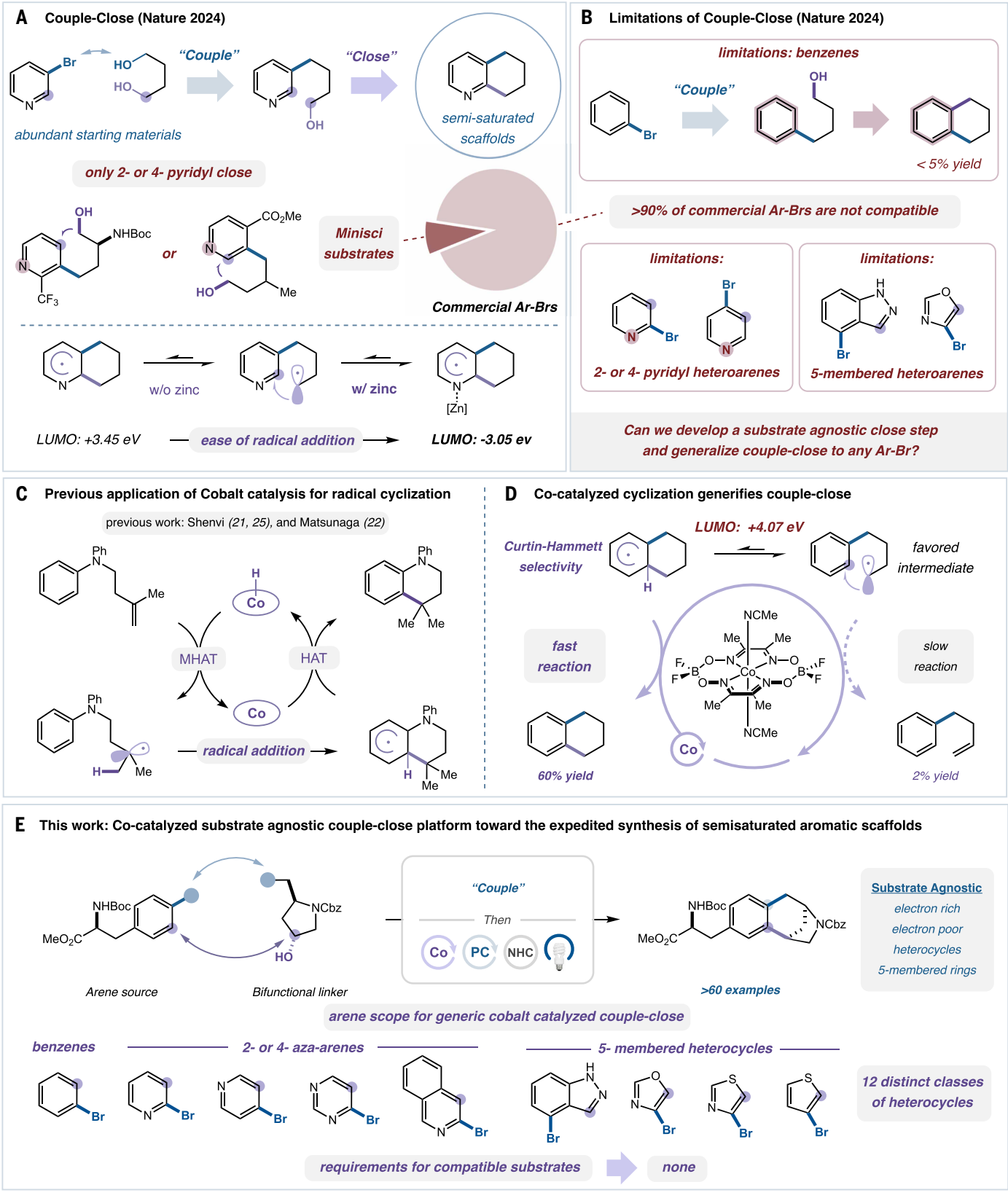

Fig. 1. Reaction design. (**A**) Couple-close (*1*) allows modular access to semisaturated scaffolds. (**B**) Initial couple-close has major scope limitations (*1*). (**C**) Previous work has shown that Co–H abstraction can drive radical cyclization from alkenes (*21*, *22*, *25*). (**D**) Cobalt-based dehydrogenation drives a favorable radical cyclization into unactivated arenes (*21*, *22*, *25*). (**E**) Accessing semisaturated arenes from a cobalt-enabled, unified couple-close platform (this work).

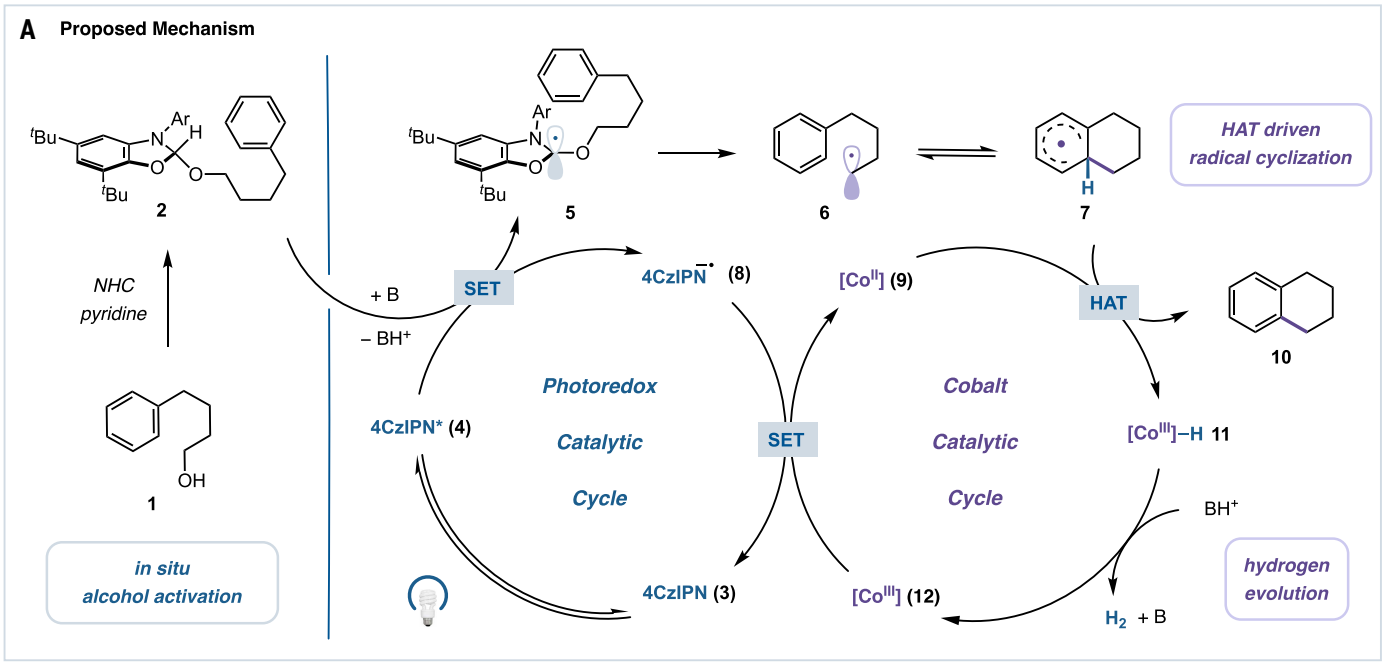

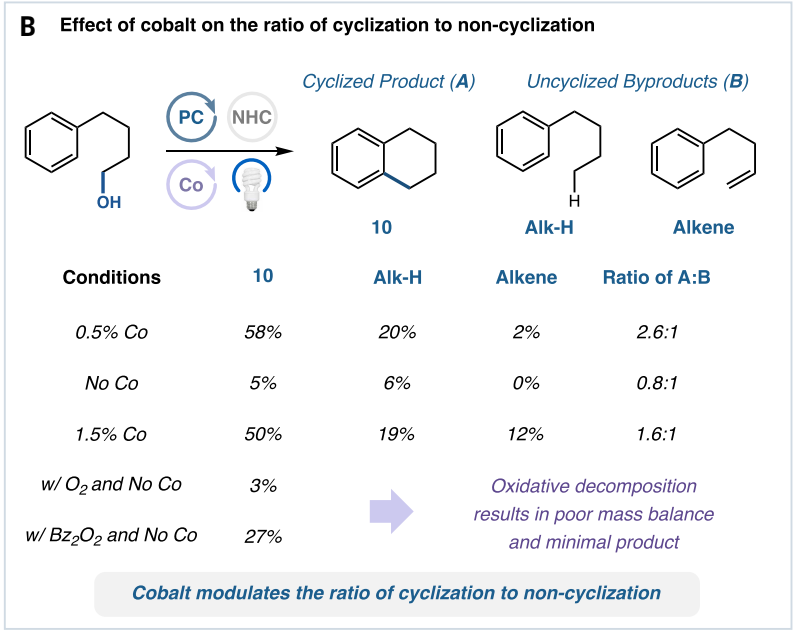

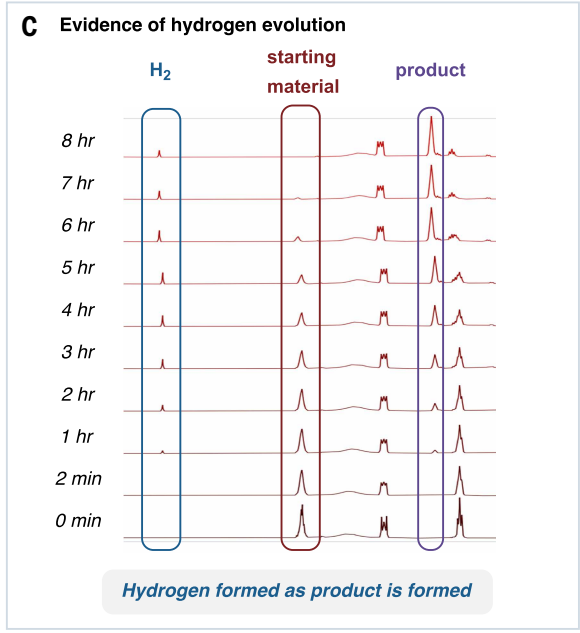

Fig. 2. Proposed mechanism. (**A**) Proposed catalytic cycle. SET, single-electron transfer. (**B**) Key role of cobalt on radical cyclization. See the supplementary materials for full experimental conditions. (**C**) PhotoNMR confirms hydrogen evolution.

radical followed by irreversible, rearomatizing deprotonation of the resulting Wheland intermediate to drive the equilibrium toward the cyclized product (*1*, *15*, *16*, *18*, *19*). This approach has been demonstrated in limited cases, but the scope remains constrained by its sensitivity to the nature of the arene substrate. In addition, these reactions often require forcing conditions, including large excesses of strong acid (*15*) or external oxidants such as peroxides (*16*), further limiting their functional group compatibility. Moreover, the driving force of the oxidation does not directly benefit from rearomatization, which only occurs after the second distinct deprotonation step. As a result, the overall efficiency of radical cyclization is highly substrate dependent and often quite poor, precluding adoption of an oxidation-deprotonation approach as a general solution to radical addition into unactivated arenes.

A general cyclization strategy would require unifying the oxidation and deprotonation steps into a single, concerted, and substrate-agnostic process. This has previously been achieved by coupling arene rearomatization to the cyclization step through removal of a hydrogen atom, thereby driving the equilibrium toward product formation (*21*, *22*, *25*). Such a mechanism could operate under milder, less-oxidizing conditions, offering a truly general solution to the longstanding challenge of radical cyclization.

In this design, concerted hydrogen atom removal from the proaromatic cyclized radical is expected to proceed independently of oxidation propensity, which generally correlates with electronic properties. We hypothesized that cobalt catalysts, which have been previously used in hydrogen evolution (*26*, *27*) and hydride HAT (*28*–*33*), might facilitate the dehydrogenation-driven radical cyclization of arenes to

generate semisaturated aromatic scaffolds (Fig. 1D). Successful realization of this strategy would require efficient radical cyclization across diverse arene electronic and steric environments, followed by cobalt-catalyzed dehydrogenation to complete the overall transformation.

Herein, we disclose a general and unified couple-close platform for the modular synthesis of semisaturated arenes driven by a cobalt-catalyzed dehydrogenation event that enables an otherwise inefficient radical cyclization (Fig. 1E). We demonstrate that abundant and readily accessible bifunctional linkers, including diols, amino alcohols, and acid alcohols, can be coupled with aryl halides, phenols, or aldehydes using a variety of established cross-coupling technologies. Subsequent alcohol deoxygenation, enabled by photoredox catalysis (*37*), generates a radical intermediate that undergoes cobalt-catalyzed dehydrogenative cyclization onto a broad range of arenes spanning 12 distinct classes of aromatic rings.

Reaction development

The cobalt-catalyzed dehydrogenative radical cyclization is proposed to proceed through the mechanism outlined in Fig. 2A. First, the alcohol (**1**) reacts with a benzoxazolium ion (NHC) to form NHC–alcohol adduct **2** (*37*). Upon blue light irradiation, a suitable photocatalyst such as 1,2,3,5-tetrakis(carbazole-9-yl)-4,6-dicyanobenzene (4CzIPN) (***3***) accesses a long-lived excited state (τ of 5.1 μs) (**4**) that is sufficiently oxidizing [$E_{1/2}^{red}$ (PC^*/PC^-) = 1.35 V versus the saturated calomel electrode (SCE)] to activate the NHC- alcohol adduct (*38*). After deprotonation by a base (B) and subsequent β-scission, a primary radical (**6**) is generated, which can reversibly add into the arene ring to form pro-aromatic radical **7**. A well-established Co(II) catalyst, Co(II)$(dmgBF_2)_2(MeCN)_2$ (**9**), mediates selective HAT with **7** (*28*–*33*) to generate a Co(III)–hydride complex, **11**, and the cyclized product **10**. Finally, the Co(III)–hydride is protonated by an acid (BH^+), generating the Co(III) complex (**12**) and releasing one equivalent of dihydrogen gas (*26*, *27*). To close the photocatalytic cycle, the 4CzIPN radical anion **8** ($E_{1/2}^{red}$ [PC/PC^-] = –1.21 V versus SCE) (*38*) reduces **12** ($E_{1/2}^{red}$ [Co^{III}/Co^{II}] = 0.2V versus SCE) (*39*), regenerating the Co(II) catalyst (**9**). Notably, the Co(II) catalyst and the base act cooperatively to mediate HAT en route to dihydrogen formation.

Our initial efforts to optimize a general couple-close strategy focused on the deoxygenative radical cyclization of 4-phenyl-1-butanol to form tetrahydronaphthalene (table S1). This model system was chosen because of its lack of Thorpe-Ingold bias and the electronic neutrality of the arene. As in our prior work, we were pleased to observe that the oxidizable NHC adduct was readily formed by simply premixing the substrate with **NHC–CF_3** in the presence of pyridine. This adduct was added, without isolation, to a solution containing the 4CzIPN photocatalyst, the Co$(dmgBF_2)_2(MeCN)_2$ dehydrogenation catalyst, catalytic base (TBAOAc), and MeCN. Upon irradiation with 450-nm light-emitting diodes for 24 hours, the desired cyclized product was obtained. Control experiments indicated that all components are necessary to ensure optimal reaction performance (for additional optimization details, see tables S1 to S12.)

In the presence of catalytic Co$(dmgBF_2)_2(MeCN)_2$, we observed the formation of the desired product in 58% yield, along with uncyclized by-products (22% combined yield), corresponding to a 2.6:1 ratio of cyclized to uncyclized product. Exclusion of Co$(dmgBF_2)_2(MeCN)_2$ resulted in a sharp decrease in yield to 5%, with uncyclized radical by-products, such as the proto-deoxygenation product arising from primary radical HAT with solvent, obtained in 6% yield, reflecting a 1:1 ratio of cyclized and uncyclized product (Fig. 2B). Extensive attempts to optimize the same cyclization under net-oxidative conditions, in which the radical cyclization step relies on an oxidation-deprotonation mechanism, were unsuccessful (table S13). This approach afforded only up to 30% yield of the desired product and very poor mass balance, consistent with oxidative substrate decomposition. These findings suggest that (i) the cobalt dehydrogenation catalyst plays a crucial role in driving the equilibrium of the reaction to the cyclized product, and (ii) cobalt-mediated dehydrogenative radical cyclization offers a milder alternative to existing strategies, enabling otherwise inefficient transformations.

Several experiments and control reactions were conducted to evaluate the proposed mechanism. Stern-Volmer analysis revealed that both NHC-alcohol adduct **2** and Co(II)$(dmgBF_2)_2(MeCN)_2$ (**9**) are competent quenchers of the excited photocatalyst. Given the 200-fold higher concentration of NHC-alcohol adduct, we propose an initial reductive quenching mechanism for the photocatalyst (fig. S6). We next sought to evaluate the ability of Co(II)$(dmgBF_2)_2(MeCN)_2$ to perform HAT from the pro-aromatic radical **7** under reaction conditions. If cobalt-mediated dehydrogenation were operative, then we would expect higher loadings of cobalt catalyst to lead to increased formation of uncyclized alkene by-products through premature dehydrogenation (*27*). Under optimal conditions with 0.5 mol % cobalt, the desired product is formed in 58% yield, whereas the alkene by-product is formed in just 2% yield (29:1 cyclized:alkene). However, increasing the cobalt loading to 1.5 mol % results in 50% yield of the desired product, along with 12% yield of the alkene by-product (4:1 cyclized:alkene) (table S7). These results strongly support the involvement of a cobalt-mediated HAT step. Finally, evolution of dihydrogen gas, consistent with turnover of the cobalt catalytic cycle, was observed in photo–nuclear magnetic resonance (photoNMR) experiments (Fig. 2C). Additional mechanistic discussion can be found in the the supplementary materials.

Scope evaluation

With optimized conditions in hand, we first explored the generality of the couple-close strategy based on the well-established metallaphotoredox deoxygenative arylation (*37*). To evaluate the scope of the reaction with respect to the arene component, a model diol derived from ribose was used as a coupling partner (Fig. 3). We were pleased to see that benzenes ranging from electron-rich and neutral (**13** to **18**) to electron-poor (**19** to **26**) underwent efficient cyclization. Notably, even highly sterically congested arenes underwent efficient "close" (**15** and **26**) and "couple" (**25**).

Next, we evaluated the scope of heterocycles that could be incorporated into the semisaturated scaffold through the couple-close sequence. We were pleased to observe that arenes capable of Minisci-type closes were competent substrates, including pyridines, pyrimidines, pyrazines, quinolines, and isoquinolines (**27** to **32**). Notably, 2-halo-pyridines and isoquinolines proved to be viable substrates, undergoing radical cyclization at the non-Minisci 3-position of the pyridine ring. Although radical addition into the 2- or 4-position of pyridines is well established (*40*), addition at the 3-position is rare because of polarity mismatching (*15*). Here, however, cobalt-catalyzed dehydrogenation is able to overcome unfavorable, polarity-mismatched radical addition, enabling cyclization at this challenging, nontraditional site (**27** and **32**). Additionally, whereas cobalt-catalyzed radical cyclization can occur with non-Minisci selectivity, traditional Minisci cyclizations are also possible, even in the absence of additional Lewis acid (**28** to **30**). Aside from 6-membered arenes and heteroarenes, this method is also capable of generating semisaturated scaffolds from 5-membered ring heterocycles, including indoles, benzothiophenes, indazoles, thiophenes, thiazoles, and oxazoles (***33*** to **38**).

The scope of the linker component was evaluated using a range of aryl and heteroaryl halides (Fig. 4). A variety of cyclic diol linkers were engaged to rapidly construct complex bridged bicyclic architectures (***39*** and **40**). In addition, primary (**41**), secondary (**42** to **45**), and tertiary (**46** to **49**) radicals were efficiently generated and cyclized, affording a diverse range of semisaturated scaffolds. The reaction exhibited broad functional group tolerance, accommodating motifs commonly found in biomolecules or useful for downstream functionalization,

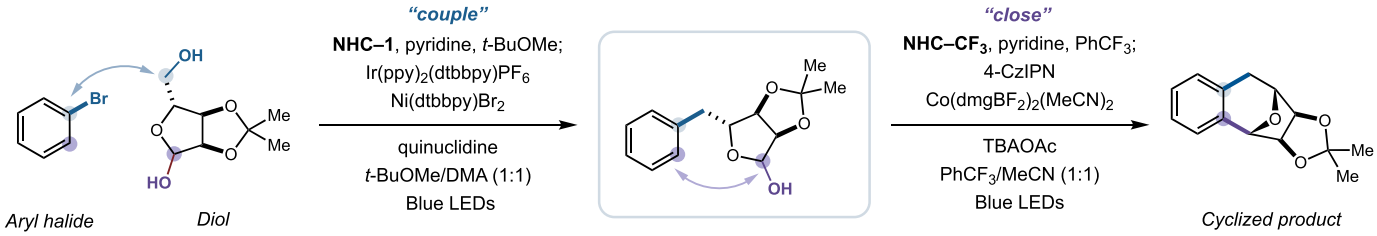

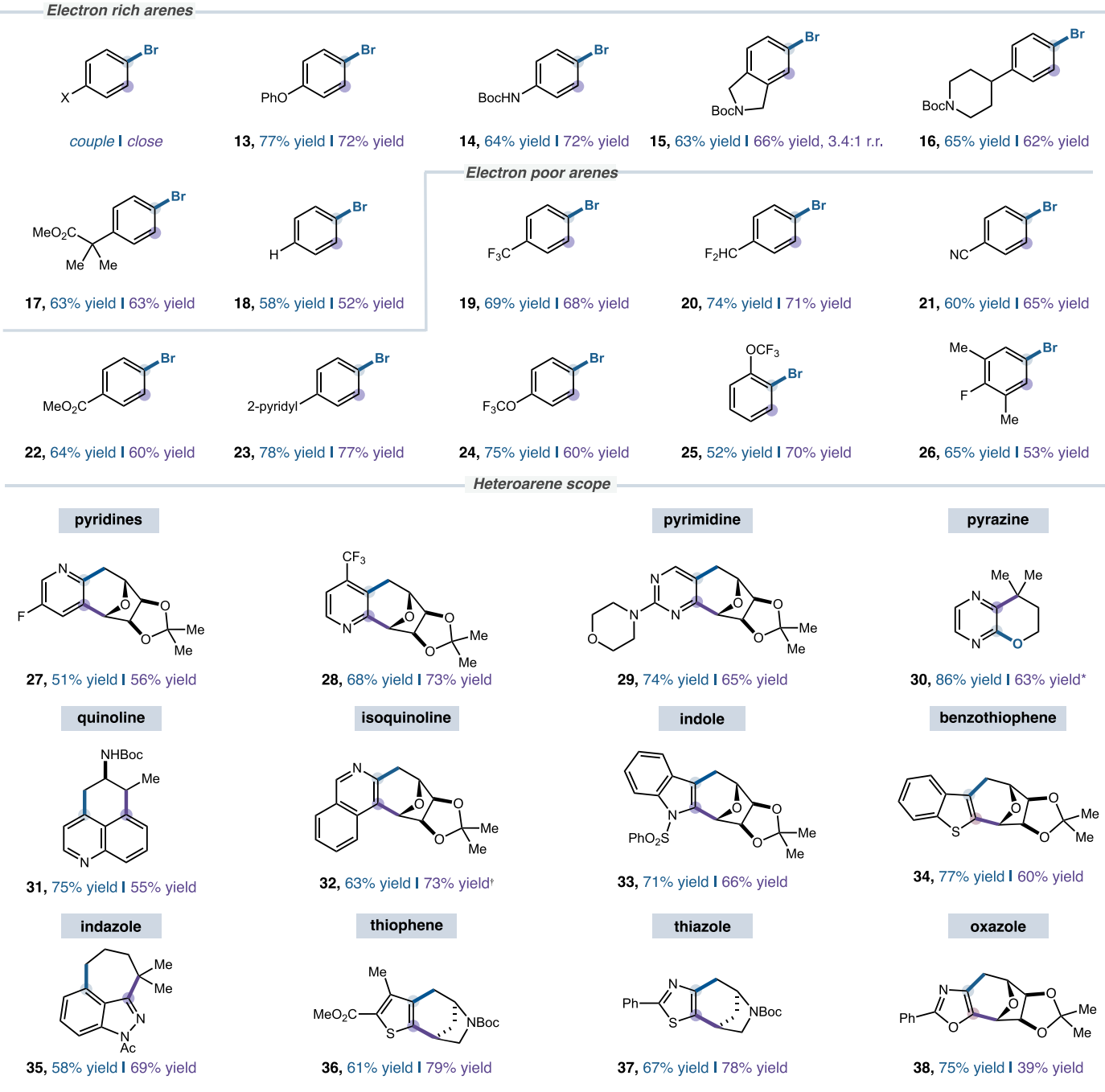

Fig. 3. Scope of deoxygenative arylation couple-close. All yields are isolated unless otherwise noted. See the supplementary materials for full detailed experimental conditions. *Couple step is S_NAR, and assay yield was determined by ultraperformance liquid chromatography–mass spectrometry (UPLC-MS) versus 1,3,5-trimethoxybenzene. †Assay yield was determined by ^{1}H-NMR versus 1,3,5-trimethoxybenzene. r.r., regioisomeric ratio.

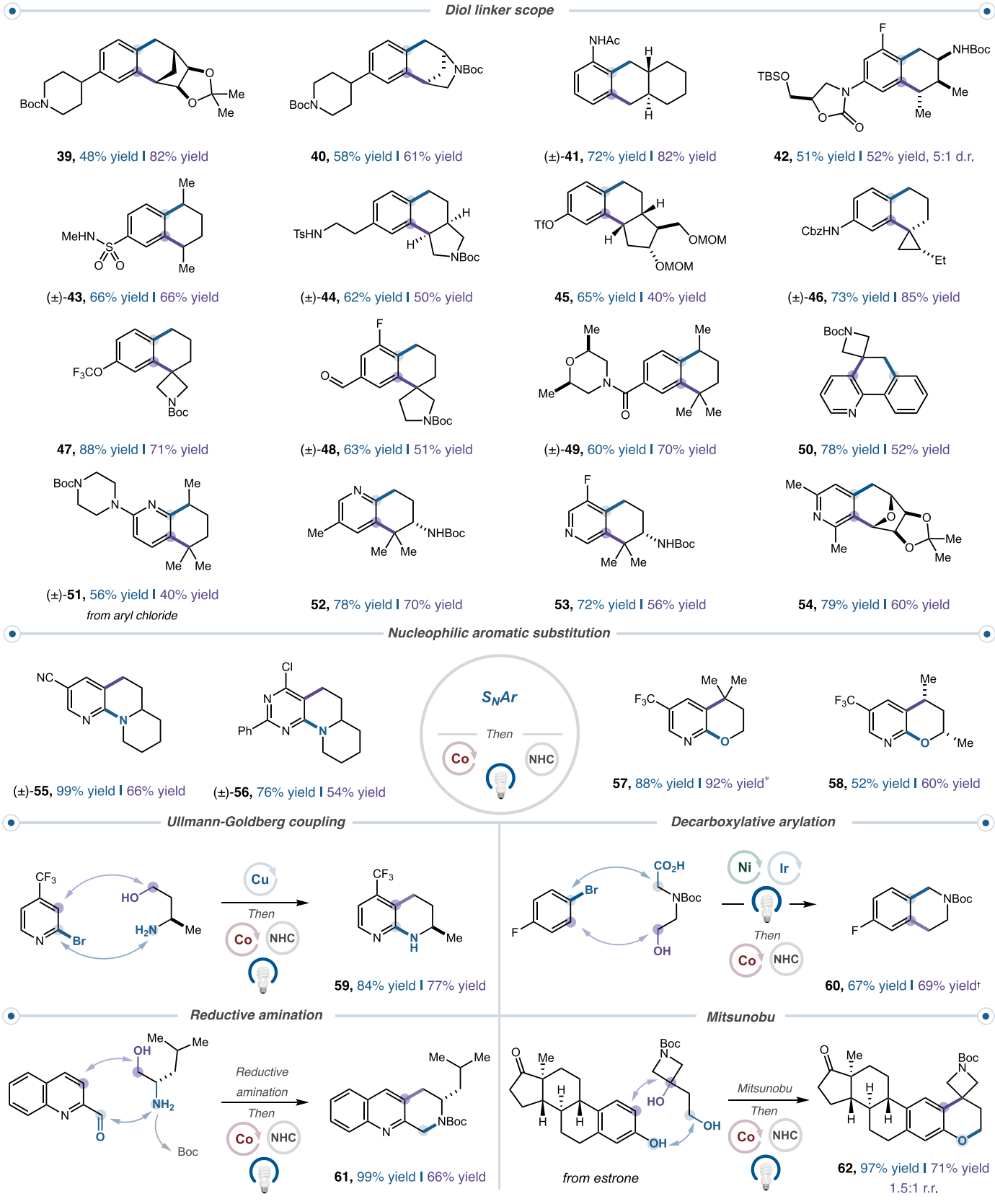

Fig. 4. Scope of alternative coupling steps. All yields are isolated unless otherwise noted. See the supplementary materials for full detailed experimental conditions. *Assay yield was determined by UPLC-MS versus 1,3,5-trimethoxybenzene. †Assay yield was determined by ^{19}F-NMR versus 1,4-difluorobenzene. d.r., diastereomeric ratio.

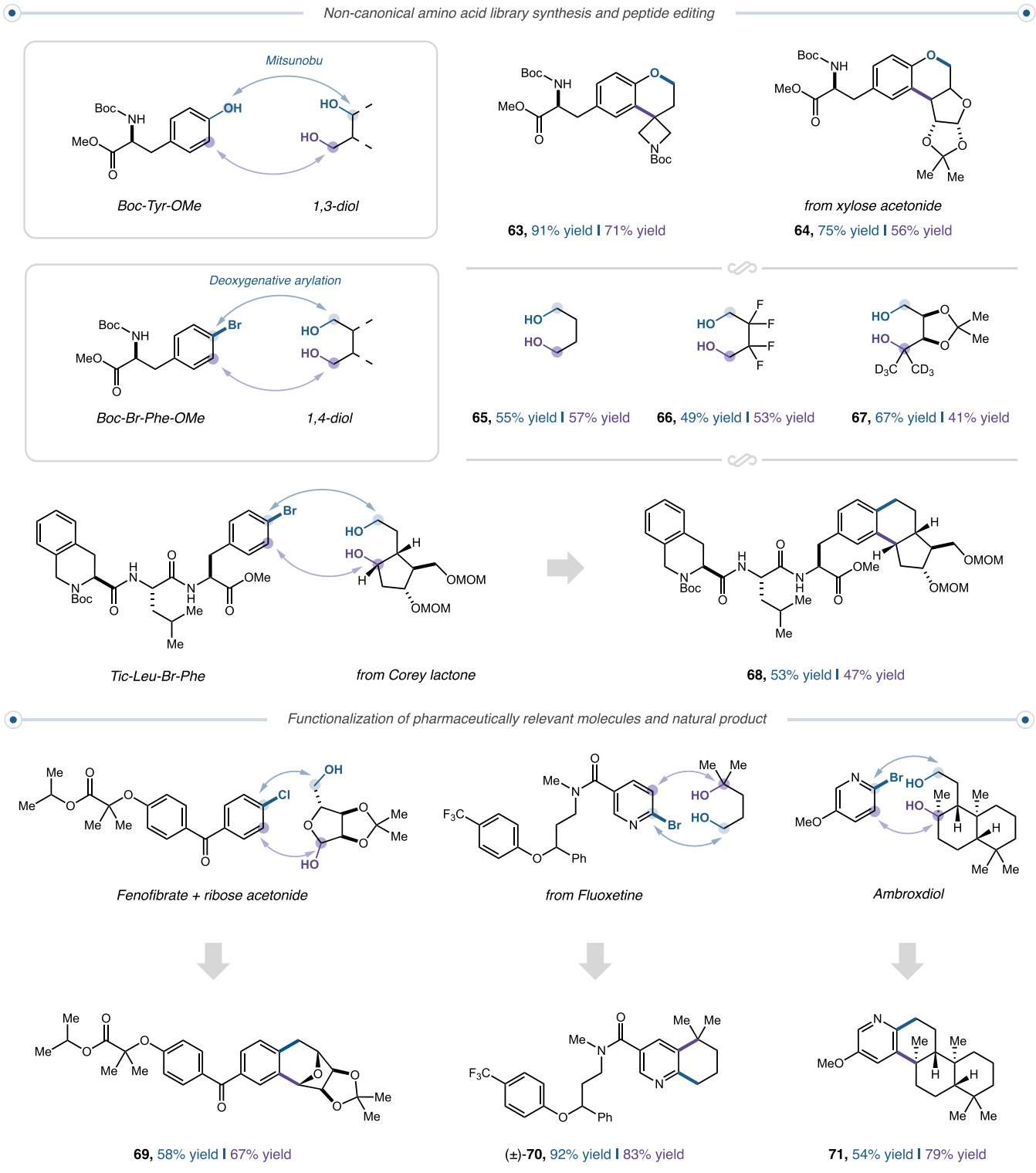

Fig. 5. Complex molecule applications. All yields are isolated. See the supplementary materials for detailed reaction conditions.

including protic functionality such as amides (**41**), protected amines (**42**), pseudohalides (**45**), sulfonamides (**43**), and aldehydes (**48**). We demonstrated that cyclization could occur "across the ring" to furnish distinct semisaturated tricyclic cores (**50**). Additionally, 2- or 4-halopyridines could also be cyclized, giving the non-Minisci adducts in good yields (**51** to **54**).

We sought to extend the couple-close platform to the construction of highly sought-after heterocycles by leveraging other classical "couple" strategies. To that end, by forging C–N or C–O bonds in the initial "couple" step, we aimed to gain rapid and modular access to pharmaceutically relevant tetrahydronaphthrydines (*41*), tetrahydroisoquinolines (*42*, *43*), and chromanes (*44*, *45*) (Fig. 4). Amino alcohols were

appended through nucleophilic aromatic substitution (S_NAr) onto electron-poor pyridines, and subsequent non-Minisci cyclization furnished tetrahydronaphthrydine ***55***. Similarly, 1,3-diols were used in a S_NAr-couple sequence to prepare 3,4-dihydro-2*H*-pyrano[2,3-b]pyridines (**57** and **58**). In cases where the S_NAr step was inefficient, copper-catalyzed Ullmann-Goldberg cross-coupling enabled the initial C–N bond formation en route to tetrahydronaphthrydine adducts (**59**). We further demonstrated that acid alcohols undergo decarboxylative arylation-cyclization (*46*, *47*) to access tetrahydroisoquinolines (**60**). Other historically robust coupling reactions also proved effective. Synthesis of tetrahydroisoquinolines (**61**) can be achieved through reductive amination, demonstrating the power of cobalt-promoted dehydrogenative radical cyclization to unify different retrosynthetic disconnections into the same synthetic outcome. Furthermore, Mitsunobu conditions facilitated coupling of phenols with diols to generate chromanes (**62**).

Finally, we evaluated the direct application of the couple-close sequence to complex biomolecules to enable the modular synthesis of unnatural amino acids (UAAs), direct modification of peptides, and functionalization of arene-containing drugs. As shown in Fig. 5, application of the couple-close platform to tyrosine provided access to chromane-containing UAAs in good yields (**63** and **64**). Bromophenylalanine and representative diols were subjected to the reaction conditions, affording semisaturated analogs with good efficiency (**65** to **67**). This strategy was further extended to more complex peptides (**68**), showcasing the power of this method to generate elaborate structurally rich scaffolds. The ability to rapidly access UAAs and modified peptides in this manner supports the development of semisaturated libraries for the discovery of therapeutic peptides with distinct pharmacological properties.

To further build on the potential of this process and challenge its bounds, we attempted late-stage modification of drug-like molecules and natural products. A range of pharmaceuticals (**69** and **70**) and natural products (**71**) were productively used as either arene partners or linkers. These results highlight the potential of this method to enable streamlined modification of advanced synthetic intermediates, thus circumventing the need for lengthy de novo synthesis and accelerating structure–activity relationship studies.

Outlook

Semisaturated bicycles are increasingly valued in drug discovery because of their distinct and enhanced properties (*1*–*9*); however, their synthesis poses a persistent challenge. Here, we report a general and unified couple-close strategy to access truly diverse semisaturated bicyclic scaffolds that features a cobalt-catalyzed dehydrogenative radical cyclization enabled by hydrogen evolution. This platform proceeds under mild reaction conditions, tolerates a wide range of functional groups, and, unlike the Minisci-based couple-close platform, is largely agnostic to the identity of the substrate. We anticipate that this platform will greatly accelerate access to previously underexplored semisaturated scaffolds and allow these motifs to be more widely represented across organic synthesis, including drug discovery programs, fine chemicals, agrochemistry, and materials science.

REFERENCES AND NOTES

1. A. Long, C. J. Oswood, C. B. Kelly, M. C. Bryan, D. W. C. MacMillan, *Nature* **628**, 326–332 (2024).
2. P. Ji *et al.*, *Chem. Soc. Rev.* **53**, 6600–6624 (2024).
3. J. Shearer, J. L. Castro, A. D. G. Lawson, M. MacCoss, R. D. Taylor, *J. Med. Chem.* **65**, 8699–8712 (2022).
4. M. Baumann, I. R. Baxendale, S. V. Ley, N. Nikbin, *Beilstein J. Org. Chem.* **7**, 442–495 (2011).
5. M. Baumann, I. R. Baxendale, *Beilstein J. Org. Chem.* **9**, 2265–2319 (2013).
6. D. G. Twigg *et al.*, *Angew. Chem. Int. Ed.* **55**, 12479–12483 (2016).
7. D.-H. Liu *et al.*, *J. Am. Chem. Soc.* **146**, 11866–11875 (2024).
8. G. Luo *et al.*, *ACS Med. Chem. Lett.* **3**, 337–341 (2012).
9. K. K.-C. Liu *et al.*, *Bioorg. Med. Chem. Lett.* **20**, 266–271 (2010).
10. P. J. Hajduk, W. R. J. D. Galloway, D. R. Spring, *Nature* **470**, 42–43 (2011).
11. A. W. Hung *et al.*, *Proc. Natl. Acad. Sci. U.S.A.* **108**, 6799–6804 (2011).
12. M. M. Heravi, V. Zadsirjan, P. Saedi, T. Momeni, *RSC Adv.* **8**, 40061–40163 (2018).
13. H. Shigehisa, T. Ano, H. Honma, K. Ebisawa, K. Hiroya, *Org. Lett.* **18**, 3622–3625 (2016).
14. E. Lunghi *et al.*, *J. Org. Chem.* **88**, 16783–16789 (2023).
15. T. C. Sherwood *et al.*, *J. Org. Chem.* **84**, 8360–8379 (2019).
16. A. Liard, B. Quiclet-Sire, R. N. Saicic, S. Z. Zard, *Tetrahedron Lett.* **38**, 1759–1762 (1997).
17. X. Zhou, Y. Xu, G. Dong, *Nat. Catal.* **4**, 703–710 (2021).
18. F. J. A. Troyano, K. Anwar, F. Mohr, G. Robert, A. Gómez-Suárez, *Eur. J. Org. Chem.* **26**, e202201176 (2023).
19. T. Saget, B. König, *Chem. Eur. J.* **26**, 7004–7007 (2020).
20. W. R. Bowman, J. M. D. Storey, *Chem. Soc. Rev.* **36**, 1803–1822 (2007).
21. J. L. M. Matos *et al.*, *Angew. Chem. Int. Ed.* **59**, 12998–13003 (2020).
22. Y. Yamaguchi *et al.*, *Org. Lett.* **24**, 2441–2445 (2022).
23. J. Tauber, D. Imbri, T. Opatz, *Molecules* **19**, 16190–16222 (2014).
24. Reaxys search 8 August 2025 comparing commercial availability of 3-bromo pyridines (24,111 commercial), quinolines (787), and pyrimidines (5015) versus bromoarenes (280,244), 2-bromo pyridines (11,892), and 4-bromo pyridines (3,329).
25. S. W. M. Crossley, F. Barabé, R. A. Shenvi, *J. Am. Chem. Soc.* **136**, 16788–16791 (2014).
26. L. A. Berben, J. C. Peters, *Chem. Commun.* **46**, 398–400 (2010).
27. J. L. Dempsey, J. R. Winkler, H. B. Gray, *J. Am. Chem. Soc.* **132**, 16774–16776 (2010).
28. S. A. Green *et al.*, *Acc. Chem. Res.* **51**, 2628–2640 (2018).
29. Ritu, D. Kolb, N. Jain, B. König, *Adv. Synth. Catal.* **365**, 605–611 (2023).
30. J. G. West, D. Huang, E. J. Sorensen, *Nat. Commun.* **6**, 10093 (2015).
31. X. Sun, J. Chen, T. Ritter, *Nat. Chem.* **10**, 1229–1233 (2018).
32. Y.-W. Zheng *et al.*, *J. Am. Chem. Soc.* **138**, 10080–10083 (2016).
33. L. Niu *et al.*, *Nat. Commun.* **8**, 14226 (2017).
34. A. Bhunia, A. Studer, *Chem* **7**, 2060–2100 (2021).
35. X.-Y. Yu *et al.*, *Adv. Synth. Catal.* **360**, 3601–3606 (2018).
36. M. J. Gibian, R. C. Corley, *Chem. Rev.* **73**, 441–464 (1973).
37. Z. Dong, D. W. C. MacMillan, *Nature* **598**, 451–456 (2021).
38. T. -Y. Shang *et al.*, *Chem. Commun.* **55**, 5408–5419 (2019).
39. X. Hu, B. S. Brunschwig, J. C. Peters, *J. Am. Chem. Soc.* **129**, 8988–8998 (2007).
40. R. S. J. Proctor, R. J. Phipps, *Angew. Chem. Int. Ed.* **58**, 13666–13699 (2019).
41. R. A. Fairhurst *et al.*, *J. Med. Chem.* **63**, 12542–12573 (2020).
42. I. Muthukrishnan, V. Sridharan, J. C. Menéndez, *Chem. Rev.* **119**, 5057–5191 (2019).
43. A. N. Kim, A. Ngamnithiporn, E. Du, B. M. Stoltz, *Chem. Rev.* **123**, 9447–9496 (2023).
44. A. García *et al.*, *Eur. J. Med. Chem.* **265**, 116125 (2024).
45. K. C. Nicolaou *et al.*, *J. Am. Chem. Soc.* **122**, 9939–9953 (2000).
46. C. N. Prieto Kullmer *et al.*, *Science* **376**, 532–539 (2022).
47. Z. Zuo *et al.*, *Science* **345**, 437–440 (2014).

ACKNOWLEDGMENTS

We thank N. Intermaggio, C. Gould, and Z. Dong for helpful scientific discussions and R. Lambert for assistance in preparing this manuscript. **Funding:** This work was supported by the National Institute of General Medical Sciences (NIGMS) of the National Institutes of Health (grant R35GM134897); the Princeton Catalysis Initiative; Johnson & Johnson Innovative Medicine; and gifts from Merck, Bristol Myers Squibb, GenMab, Genentech, and Pfizer. W.Y.Z. acknowledges Princeton University for a first-year fellowship. This material is based upon work supported by the National Science Foundation Graduate Research Fellowship Program under grant DGE-2444107 to W.L.L. Any opinions, findings, and conclusions or recommendations expressed in this material are those of the authors and do not necessarily reflect the views of the National Science Foundation. **Author contributions:** J.X. and D.W.C.M. conceived of the work. All authors designed the experiments. J.X., W.Y.Z., N.T., W.L.L., J.Z.W., and A.L. performed the experiments. J.Z.W. and D.W.C.M. prepared the manuscript with input from all authors. **Competing interests:** D.W.C.M. declares a financial interest with respect to the Integrated Photoreactor. The remaining authors declare no competing interests. **Data, code, and materials availability:** Data are available in the supplementary materials.

SUPPLEMENTARY MATERIALS

science.org/doi/10.1126/science.aec5748
Materials and Methods; Figs. S1 to S17; Tables S1 to S19; References (*48*–*58*); NMR Spectra

Submitted 24 September 2025; accepted 8 December 2025

10.1126/science.aec5748

Couple-close: Unified approach to semisaturated cyclic scaffolds

Jiaxin Xie, William Y. Zhao, Johnny Z. Wang, William L. Lyon, Noriyuki Takanashi, Alice Long, Taylor M. Sodano, Christopher B. Kelly, Marian C. Bryan, and David W. C. MacMillan

Science **391** (6783), . DOI: 10.1126/science.aec5748

Editor's summary

Many of the most efficient reactions currently used in pharmaceutical research link together flat molecular fragments. Finding ways to diversify structures in the third dimension is thus a burgeoning area of research. Xie *et al*. report a versatile method of fusing flat aromatic rings to nonplanar saturated counterparts. After tethering one end of the saturated backbone to the aromatic cycle, the authors used a cobalt catalyst together with a photoredox catalyst to close the second ring, releasing hydrogen as a by-product. —Jake S. Yeston

Science (ISSN 1095-9203) is published by the American Association for the Advancement of Science. 1200 New York Avenue NW, Washington, DC 20005. The title *Science* is a registered trademark of AAAS.